

Use of Raman scattering to investigate disorder and crystallite formation in as-deposited and annealed carbon films

R. O. Dillon* and John A. Woollam

Department of Electrical Engineering, University of Nebraska, Lincoln, Nebraska 68588
and

V. Katkanant

Department of Physics, University of Nebraska, Lincoln, Nebraska 68588

(Received 5 July 1983)

Carbon films were prepared by ion-beam as well as rf-discharge deposition, and annealed at temperatures up to 950 °C. Raman spectra of these films, in the range 1000–1800 cm^{-1} , were analyzed via a best fit to computer-generated line shapes, used to simulate the *D* and *G* lines. Our results are given in terms of the $I(D)/I(G)$ intensity ratio, line position, and linewidth as a function of anneal temperature. The $I(D)/I(G)$ ratio for the rf-discharge-deposited films shows a maximum, and there is a suggestion of similar behavior for the ion-beam-deposited films. This maximum indicates that crystallite growth is promoted by higher anneal temperatures. As suggested by comparison with theory, the down-shifted *G* line position of 1536 cm^{-1} in the as-deposited films indicates the presence of bond-angle disorder. The similarly, down-shifted *D* line position of $\sim 1283 \text{ cm}^{-1}$ indicates that the as-deposited films may contain some fourfold-coordinated bonds as well as disorder. The shift of the *D* and *G* lines to asymptotes of 1353 and 1598 cm^{-1} , respectively, as anneal temperature increases, indicates that the crystallites are dominated by threefold over fourfold coordination. The linewidths of both lines decrease in width with increasing anneal temperature. This is also consistent with the removal of bond-angle disorder and the increasing dominance of crystallites as annealing proceeds to higher temperatures.

I. INTRODUCTION

Carbon has two crystalline forms, graphite (with threefold-coordination symmetry) and diamond (with fourfold-coordination symmetry). For both structures the Raman spectra are well known.^{1–3} The first-order Raman spectrum of diamond consists of a single line at 1332 cm^{-1} . The corresponding spectrum of large single-crystal graphite also has a single high-frequency line, the “*G*” line at about 1580 cm^{-1} .

Raman spectra are very sensitive to changes that disrupt the translational symmetry of the material studied, as occurs in small-dimensional crystals. Carbonaceous materials can be prepared with a wide range of crystallite sizes.^{1–3} The most striking feature of the Raman spectrum of small graphite crystallites (basal plane dimensions $\leq 200 \text{ \AA}$) is the appearance of an additional disorder, or “*D*”, line, at about 1355 cm^{-1} . A secondary feature is that changes occur in the region of the *G* line. Some workers³ report that the *G* line moves slightly upward in frequency, while others⁴ claim that the *G* line is stationary, but a new line, the *D*' line, appears at about 1613 cm^{-1} .

These changes in the Raman spectrum can be explained by reference to the phonon density of states for graphite shown in Fig. 1, from Al-Jishi and Dresselhaus.⁵ As long-range translational symmetry is lost, crystal momen-

tum need no longer be conserved, and phonons with any \vec{k} vector throughout the Brillouin zone may contribute to the Raman spectrum. The spectrum for disordered materials favors phonons associated with large electron-phonon-coupling constants as well as those associated with large densities of phonon states. The appearance of the *D* line and the upward shift of the *G* line (or appearance of the *D*' line) is then explained by large density-of-states peaks at $k \neq 0$ points in the Brillouin zone. As all \vec{k} -vector optical phonons can now contribute to Raman scattering, other, more subtle changes in the spectrum may occur as well. For example, other lines may be seen at about 1230 and 870 cm^{-1} as well as at lower frequencies.

Raman spectra sensitive to changes in translational symmetry are thus useful for the study of disorder and crystallite formation in thin carbon films. We have been making amorphous films by ion-beam sputtering and rf plasma deposition. For such films the long-range translational symmetry may also be lost by introducing bond-angle disorder into the film. Recent calculations by Bee-man⁶ appropriate for carbon films indicate that this disorder produces effects on the Raman spectra quite different from the effects produced by small graphite crystallites. He built computer models containing up to 1120 carbon atoms and used simple force-constant approximations to calculate Raman spectra. Using threefold bonding

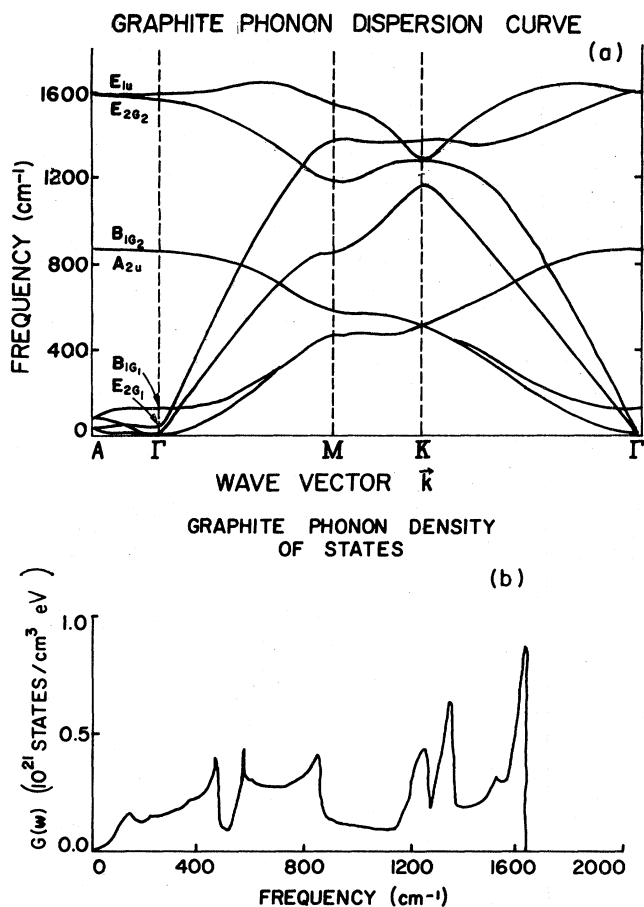


FIG. 1. (a) Phonon dispersion curves for graphite, and (b) phonon density of states (Ref. 5).

without bond-angle disorder, Beeman correctly produced the graphite G line near 1581 cm^{-1} , but his D line was low in frequency, appearing at 1310 cm^{-1} .

As Beeman changed the bond angle from the ideal 120° to a disordered average of $117.7^\circ \pm 5.0^\circ$, the G line shifted down to 1528 cm^{-1} , while the D line remained at 1310 cm^{-1} . Then, in a model assuming certain percentages of fourfold-coordinated atoms and bond-angle disorder, both peaks shifted down in frequency, with the G -line shift approximately linear with increasing percentage of fourfold-coordinated atoms. Even when his model assumes 51% fourfold-coordinated atoms, no major features appeared at the 1332-cm^{-1} Raman peak found in diamond.

This downshift of Raman peaks with disorder and fourfold coordination is relevant because a downshift of the G peak is evident in earlier work. A study of Lannin's⁷ weighted, reduced Raman spectrum for an as-deposited film indicates that the G line is at about 1530 cm^{-1} . The work of Wada *et al.*⁸ also indicates a downshift of the G line associated with an as-deposited film. The peak position associated with the film of Wada *et al.* was identified by Solin *et al.*⁹ to be 1520 cm^{-1} . In addition, a downshift of the G line was noted by Elman *et al.*¹⁰ in graphite ion-implanted to high fluences.

In this paper we report on Raman data on amorphous carbon films deposited by rf plasma deposition and by

ion-beam-sputter deposition. These materials are sometimes reported as being hard, semitransparent (band gap up to 3 eV), and chemically inert.¹¹ We have studied the Raman spectra of these films as-deposited, and annealed them in steps up to 950°C . We see several trends and features consistent with the as-deposited films being amorphous with bond-angle disorder, with threefold-coordinated crystallites forming as annealing proceeds.

II. EXPERIMENTAL

Two techniques were used to deposit carbon films. One method used ion-beam sputtering of a carbon target with argon ions and had a deposition rate of $10\text{--}15\text{ \AA}/\text{min}$. The other method used a Perkin-Elmer model-3140 sputtering system in the "etch" mode. Methane gas was introduced and about 20 W of rf power was used to produce a discharge. Deposition rates of approximately $100\text{ \AA}/\text{min}$ were measured with this system.

Two complete runs, numbered 1 and 2, were performed on room-temperature substrates which were first sputter-cleaned with argon ions in both techniques. Most of the films were deposited on silicon wafers, but a few were also deposited on sapphire substrates. The films from run no. 1 were annealed for 0.5 h in hydrogen at temperatures ranging from 550 to 950°C , while those from run no. 2 were annealed for the same time in nitrogen from 200 to 950°C .

Raman spectroscopy was performed by backscattering from the sample using an argon-ion laser operating at 5145 \AA at a power of 180 mW. First-order Stokes spectra were detected with a Spex double monochromator, usually scanned between 1000 and 1800 cm^{-1} . These spectra were then analyzed quantitatively using a computer to reproduce the data as a sum of two lines each given by the expression from DiDomenico *et al.*,¹²

$$\frac{dI}{d\omega} \propto \frac{\Gamma\omega_0}{(\omega_0^2 - \omega^2)^2 + 4\Gamma^2\omega_0^2\omega^2}, \quad (1)$$

where $dI/d\omega$ is proportional to the detector signal at ω , ω_0 is the undamped mode frequency, ω is the frequency shift from the laser line, and Γ is a damping constant. Computer fits to the data determined ω_0 and Γ for each peak, and then an integration of (1) gave the integrated intensity I associated with each peak.

III. RESULTS

Figure 2 shows the change in the spectra as a function of anneal temperature for run no. 2 (ion-beam-sputter deposited) films. Two important features are (1) the increase of D -line-to- G -line intensity ratios $I(D)/I(G)$ with anneal temperatures up to about 600°C , and (2) the upward shift of the G line that occurs up to anneal temperatures of about 600°C , with the G line remaining approximately constant in frequency for higher anneal temperatures. The spectra in Fig. 2 are similar to those observed by Wada *et al.*⁸ for sputtered films annealed up to 500°C in vacuum. In addition, we observe a narrow line at 1120 cm^{-1} , the origins of which are not known. While the rest of the spectra remained constant, this narrow line

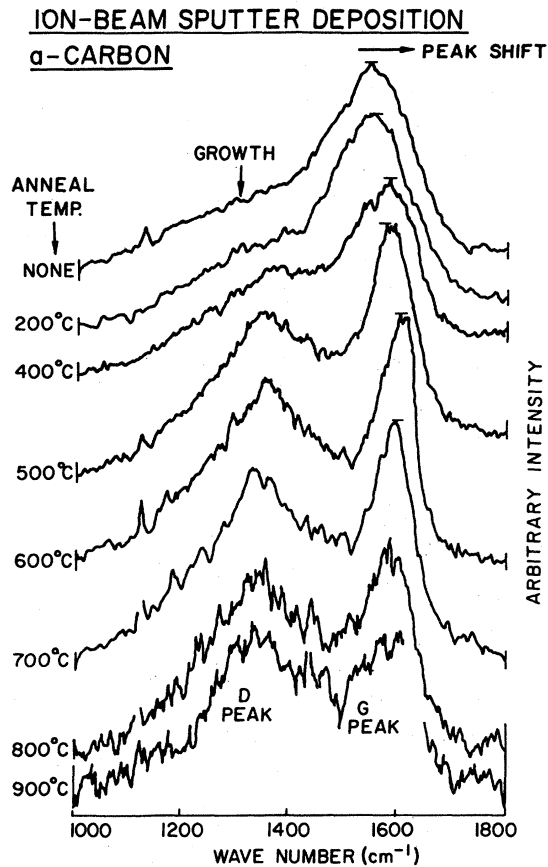


FIG. 2. Raman spectra for a series of anneal temperatures up to 900°C in an ion-beam-sputter-deposited sample.

varied by a factor of 2 in amplitude as a second scan was taken of a particular film. In addition, it did not appear in preliminary spectra of similar films or of a bare silicon

substrate using either 4880- or 5145-Å laser wavelengths.

Excellent computer fits to the data were obtained for the as-deposited and 200 and 400°C annealed samples. Beginning at about a 500°C anneal temperature, the data had a greater amplitude (which we define as "excess amplitude") than the computer reproduction, based on a two-oscillator model in broad regions around 1200 and 1500 cm^{-1} . This trend continued for the higher anneal temperatures. Also, at about 500°C the high-frequency side of the G line began to fall off faster than the computer reproduction, and this was also observed at most higher anneal temperatures. (These facts are discussed in Sec. IV.)

Figure 3 shows the $I(D)/I(G)$ intensity ratio as a function of anneal temperature for the two rf depositions, including one point derived from spectra taken at 77 K. The intensity ratios were calculated analytically using the result of an integration over Eq. (1) given in DiDomenico *et al.*¹⁰ The $I(D)/I(G)$ ratio does not appear to be influenced by the gas used in the annealing chamber or by the substrate used for the deposition. The rise in intensity ratio with anneal temperature up to about 800°C is a continuation of the trend evident in Fig. 2. However, the use of the computer reproductions and high anneal temperatures allowed us to observe (for the first time), a decrease in $I(D)/I(G)$ as a function of anneal temperature. As will be discussed later, large uncertainties are associated with the width of the G line at very high anneal temperatures and this is also reflected in the $I(D)/I(G)$ ratio. A calculation made with the smallest permissible width for the G line at 950°C raised the corresponding $I(D)/I(G)$ ratio from 1.15 to 1.57. Even at 1.57, a decline is indicated, thus verifying that the decrease in intensity ratio at high anneal temperature is a real phenomenon.

Figure 4 shows the intensity ratio for the two ion-beam depositions, including some data taken with the sample at

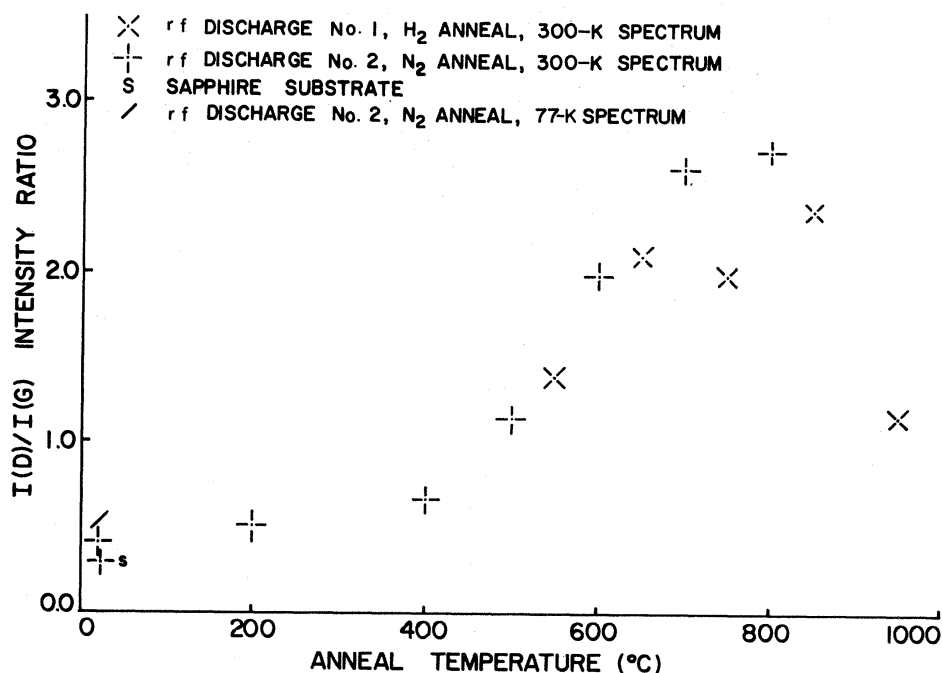


FIG. 3. Intensity ratio vs anneal temperature for a series of rf-discharge-prepared samples.

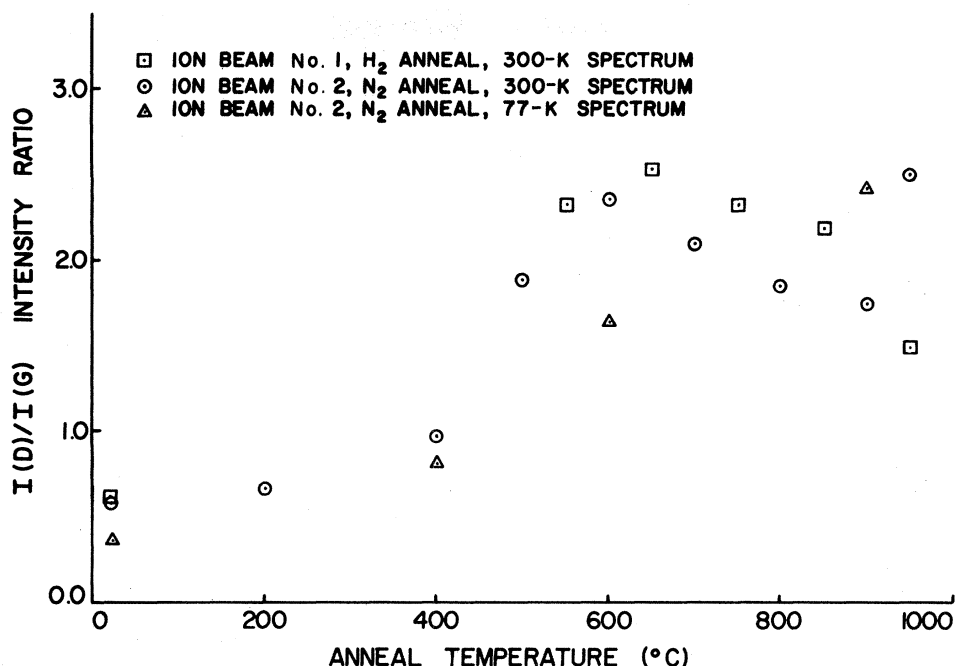


FIG. 4. Intensity ratio vs anneal temperature for a series of ion-beam-sputter-deposited samples.

77 K. Six of eight data points above 650°C indicate a decrease of $I(D)/I(G)$ with increasing anneal temperature. Electron spectroscopy for chemical analysis carried out on these films shows that the high data point at 950°C corresponds to a film that was contaminated with gallium (also, the 700°C data point corresponds to a sample contaminated with barium), and so this point must be viewed with suspicion.

Figure 5 shows the shift of the G line from about 1536 cm^{-1} to about 1598 cm^{-1} for both runs, and again includes some data taken while the films were at liquid-

nitrogen temperature. The upward shift toward 1598 cm^{-1} occurs more rapidly for the ion-beam-sputter-deposited films than those deposited with rf discharge; however, both reach the same asymptote for temperatures greater than 500–550°C. The change from room temperature to liquid-nitrogen temperature in taking the Raman spectra did not systematically change the line positions.

The use of the computer program was essential in extracting data for the position of the D line with anneal temperature, and this is probably the reason the data in

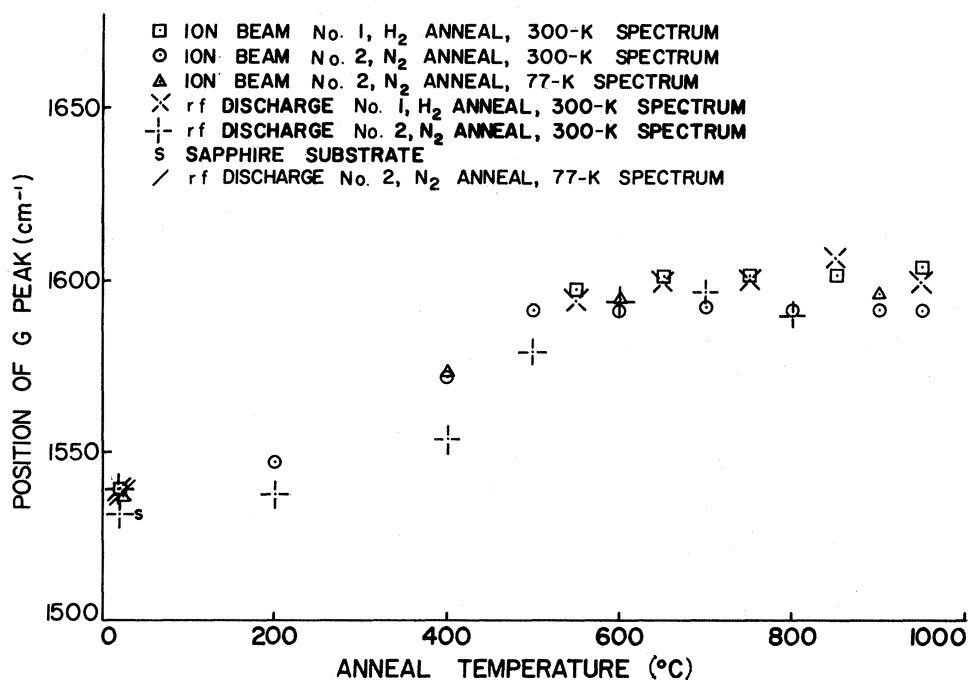


FIG. 5. Position of G peak vs anneal temperature.

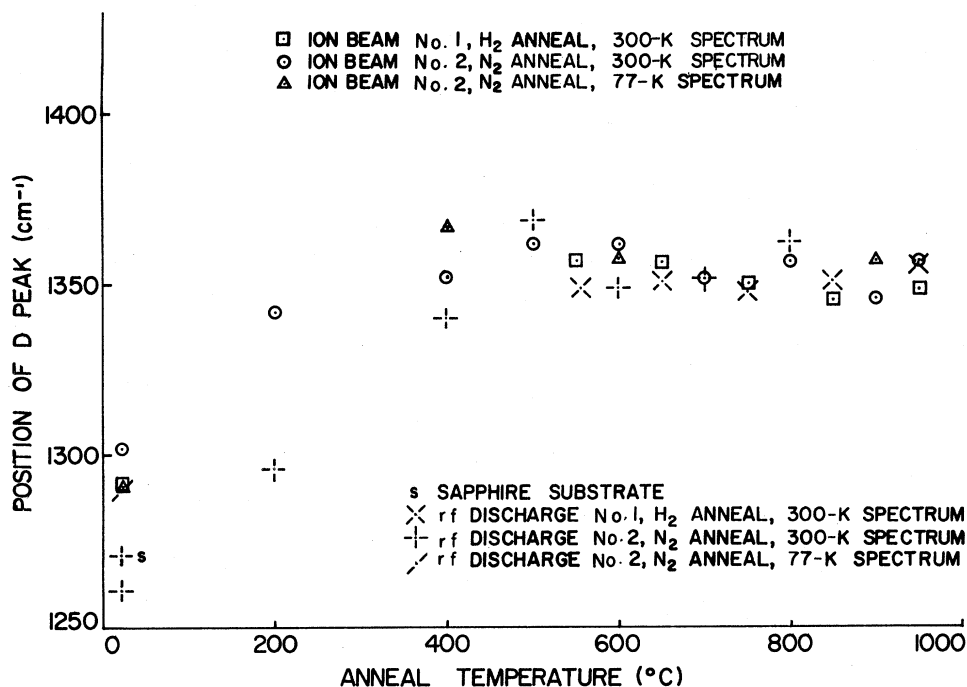
FIG. 6. Position of *D* peak vs anneal temperature.

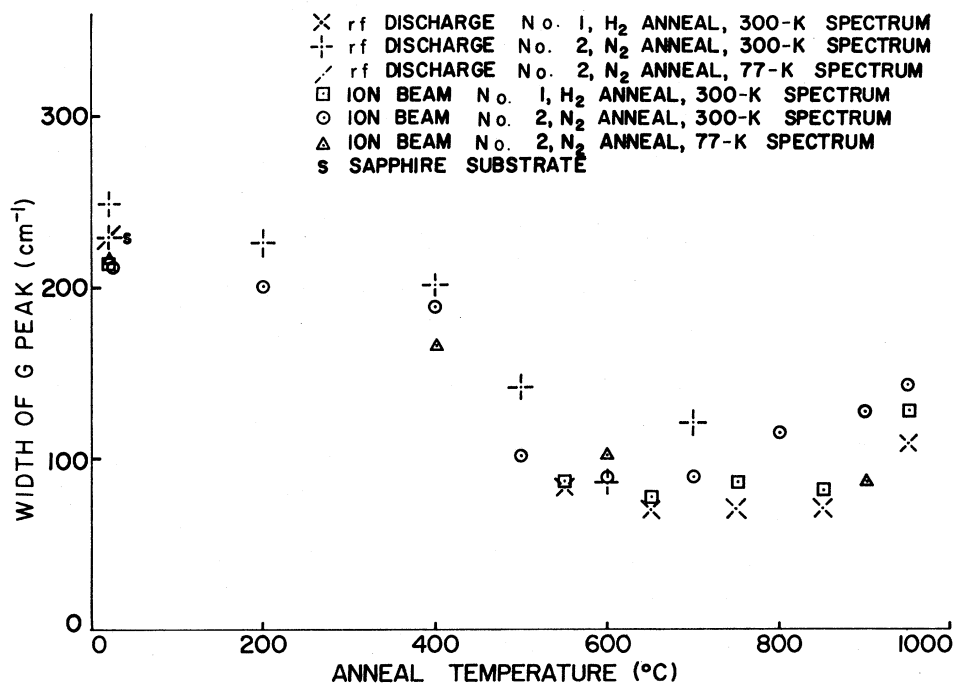
Fig. 6 has not been previously reported. As in Fig. 5, the films made via ion-beam deposition show higher *D*-line frequencies at low anneal temperatures than those made with rf discharge. However, Fig. 6 shows that this difference of *D*-line position also occurs in the as-deposited films. That is, including data at liquid-nitrogen temperature, the average of the three as-deposited rf positions is 1271 cm^{-1} , while the corresponding average for the ion-beam-deposited films is 1295 cm^{-1} . The *D* line for both

types of films reaches the same asymptote, $\sim 1353\text{ cm}^{-1}$, for anneal temperatures greater than $400\text{--}500^\circ\text{C}$.

The variation of the width [full width at half maximum (FWHM)] of the *G* line as a function of anneal temperature is shown in Fig. 7. The widths were calculated from

$$\Delta\nu(\text{FWHM}) = 2\omega_0\Gamma, \quad (2)$$

which gives results for the data shown to within 1% of the values derived by solving the quartic equation implied

FIG. 7. Width of *G* peak vs anneal temperature.

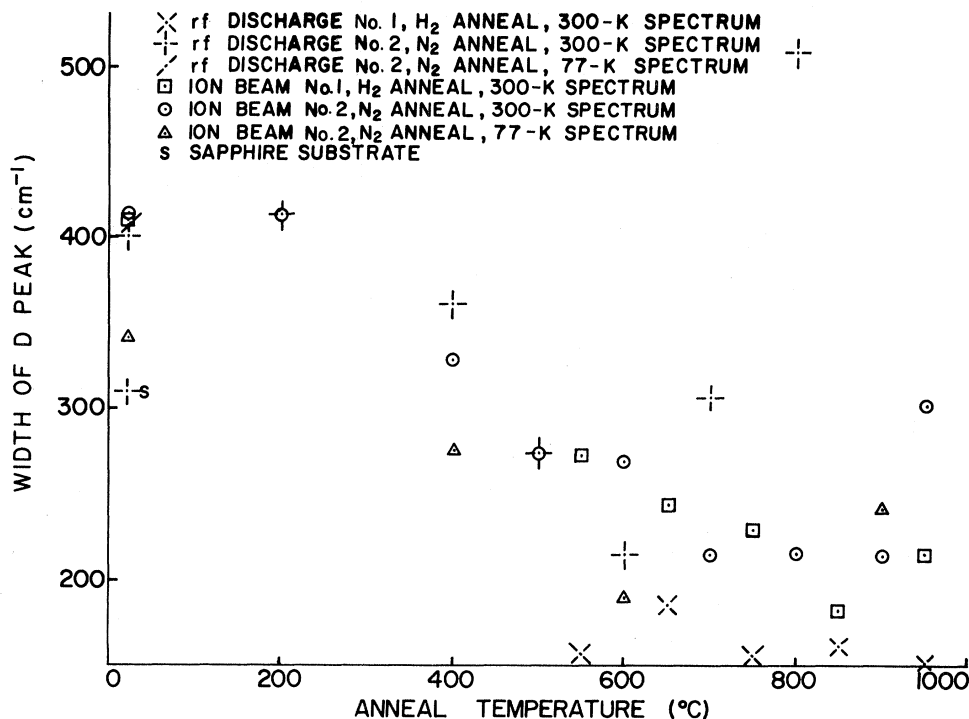


FIG. 8. Width of D peak vs anneal temperature.

in (1) for the width. Again, a difference exists between the ion-beam-deposited and rf-deposited films for low anneal temperatures and in the as-deposited state. In particular, the G line is consistently wider for the rf-deposited films than it is for the ion-beam-deposited films, up to an anneal temperature of about 550°C. The linewidth is approximately constant from 550 to 800°C, and then an increase in width is indicated at 900–950°C. However, the linewidth at these highest anneal temperatures is very difficult to determine. As the G line becomes weak at these anneal temperatures, it is hard to judge what part of the amplitude around 1500 cm^{-1} is associated with the G line and what part is the usual excess amplitude which is not reproduced by the computer. Thus, we cannot tell whether the indicated width increase is a “real” effect or is a function of the manner in which we have fit the computer reproduction to the data. However, with the exception of these high-temperature points, the overall trend is a decrease in the G linewidth as anneal temperature is raised, with the most rapid decrease occurring at about 500°C.

Figure 8 shows the width of the D peak as a function of anneal temperature. For widths of less than 275 cm^{-1} , the approximate Eq. (2) was used, again giving results within 1% of the true calculated values. For widths larger than 275 cm^{-1} , the appropriate quartic equation from (1) was solved, giving results about 10 cm^{-1} larger than those based on (2) at 400 cm^{-1} . The scatter in the data points is considerably larger than in Fig. 7 for the G line. This is partially because, for low intensities, it is more difficult to judge the width of a wide line than a narrow one. In Fig. 8 there are four sets of data with enough data points plotted to see trends. All films except the rf-deposited films annealed in hydrogen exhibit an overall decrease in width as anneal temperature is raised, followed

by an increase in width at the highest anneal temperatures. Similar to the G linewidths, the upturn at high temperatures may be due to the inclusion of excess amplitude at around 1200 cm^{-1} as the signal weakens, although the behavior of the rf-deposited films annealed in nitrogen suggest that this upturn is a real effect.

IV. DISCUSSION

In the sections above we described Raman intensity and frequency changes with annealing. In this section these results will be discussed, especially within the context of proposed structural models.

The rise of the $I(D)/I(G)$ intensity ratio with anneal temperature in Figs. 3 and 4 is consistent with a model which predicts a growth in number and/or size of crystallites, as will now be explained. This ratio is roughly proportional to the ratio of momentum nonconserving-to-conserving phonons which contribute to the Raman spectrum. Very small crystallites probably exist in the film at low annealing temperatures, but because of their small size and number, they are only weakly coupled to the incoming laser beam, and thus contribute little to the Raman spectrum. As the annealing temperature is increased, the crystallites grow in size and/or number, and thus they begin to contribute to the Raman spectrum, causing the $I(D)/I(G)$ ratio to increase. If the crystallites increase in number only, then this model is similar to that of Wada *et al.*,⁸ whereby planar clusters of random-network carbon atoms with dimensions of about 20 Å crystallize as the annealing temperature is raised.

The development of a maximum in the $I(D)/I(G)$ ratio in carbons as a function of anneal temperature is well known and has been noted by Vidano and Fishbach,¹³ for

example, for many types of carbons including glassy carbons and carbon fibers. If the intensity ratio goes to zero at high anneal temperature, then Vidano and Fischbach¹³ state that graphitization has occurred. Thus we interpret the decrease of the $I(D)/I(G)$ ratio to an increase in the dimensions of crystallites above some annealing temperature. As the crystal grows, the effects of momentum conservation begin to increase in importance (since momentum is conserved in a large crystal), and thus the $I(D)/I(G)$ ratio starts to decline.

With the aid of x-ray diffraction, Tuinstra and Koenig³ established a linear relationship between the magnitude of $I(D)/I(G)$ and inverse crystallite size. Since crystal-size effects must cause the decrease of our $I(D)/I(G)$ curve, we can apply this relationship to the decreasing portion of our graph. This yields crystallite sizes of 16 and 38 Å for the films annealed at 800 and 950°C, respectively. The 16-Å size agrees well with the 20-Å crystallite size before growth commences estimated by Wada *et al.*⁸

We propose that the as-deposited films contain bond-angle disorder as given in Beeman's model.⁶ The line positions thus yield information concerning bond-angle disorder and the bonding in the crystallites that form. Bond-angle disorder seems to be the only mechanism capable of down-shifting the lines to the extent that we observe, and also the observed average G -line position at 1536 cm^{-1} is close to the value of 1528 cm^{-1} predicted by Beeman.⁴ According to his model, the low average values of 1271 and 1295 cm^{-1} for the D line of the rf-deposited and ion-beam-deposited films, respectively, may require the presence of some fourfold-coordinated bonds as well as disorder. The asymptotes of 1353 and 1598 cm^{-1} for the D and G peaks as a function of anneal temperature, indicate that the crystallites formed at high temperature are threefold coordinated. That is, these asymptotes are consistent with the lines observed from small crystallites of graphite.

The shift of the G line from 1580 to 1598 cm^{-1} indicates that phonons near the high-frequency end of the phonon density of states (see Fig. 1) are active in Raman scattering when the $k=0$ rule is relaxed. However, from Fig. 1, the expected asymptote is nearer to 1620 cm^{-1} than the observed value of 1598 cm^{-1} . The very abrupt drop in the density of states at the high-frequency end is the reason the G line decreased faster than the computer reproduction. It should be noted that Eq. (1) produces an asymmetric line shape with a more rapid decline on the

high-frequency side of the peak. Examination of the density of states (neglecting variations in the electron-phonon interaction) near the D and G lines shows that this function should fit the data better than a symmetric line shape. The observed asymptote value of 1353 cm^{-1} indicates that this line originates from the second-highest peak in the density of states. The excess amplitudes noted at 1200 and 1500 cm^{-1} are probably due to the overall rise in the density of states beginning just before 1200 cm^{-1} and continuing to 1620 cm^{-1} .

The decrease in linewidth observed for the D and G lines as anneal temperature is increased is consistent with the removal of bond-angle disorder and the increasing dominance of crystallites. The linewidths are very large in the as-deposited films because of the bond-angle disorder. The line then narrows as the disorder is removed by annealing and as crystallites become more dominant.

In summary, the graphs of $I(D)/I(G)$, and of peak width versus anneal temperature, indicate that substantial structural changes occur over the 400–600°C anneal-temperature range. The direction of the change suggests a growth in number or size of crystallites at these temperatures. The decrease in the $I(D)/I(G)$ data at higher anneal temperatures then indicates a growth in crystallite dimensions. The crystallites are identified as threefold coordinated because of the shift in line positions toward graphitelike values. As substantial shifts of the D line are evident at anneal temperatures less than 400°C, these shifts are the most sensitive indications that the films are changing from ones with bond-angle disorder to ones containing threefold-coordinated crystallites as annealing proceeds.

ACKNOWLEDGMENTS

We would like to thank Bruce Banks and Stan Domitz of the National Aeronautics and Space Administration (NASA) Lewis Research Center for their kind hospitality in preparation of the films used for these experiments. Useful conversations were held with David Beeman, and we wish to thank him for showing us his results prior to publication. We would especially like to thank Frank Ullman, John Hardy, and Roger Kirby for helpful discussions and use of their Raman scattering facility. This research was supported in part by grants from the NASA Lewis Research Center, Cleveland, Ohio, and the Nebraska Research Council.

*On leave from the Department of Physics, University of Waikato, Hamilton, New Zealand.

¹P. Lespade, R. Al-Jishi, and M. S. Dresselhaus, *Carbon* **20**, 427 (1982).

²R. Vidano and D. B. Fishbach, *J. Am. Ceram. Soc.* **61**, 13 (1978).

³F. Tuinstra and J. L. Koenig, *J. Chem. Phys.* **53**, 1126 (1970).

⁴H. Maeta and Y. Sato, *Solid State Commun.* **23**, 23 (1977).

⁵R. Al-Jishi and G. Dresselhaus, *Phys. Rev. B* **26**, 4514 (1982).

⁶D. Beeman, M. R. Anderson, J. Silverman, and R. Lynds (unpublished).

⁷For data on Raman scattering in amorphous C, MoS₂, and

GaSe, see J. S. Lannin, in *Proceedings of the 7th International Conference on Amorphous and Liquid Semiconductors, Edinburgh, Scotland, 1977*, edited by W. E. Spear (University of Edinburgh Press, Edinburgh, 1977).

⁸N. Wada, P. J. Gaczi, and S. A. Solin, *J. Non-Cryst. Solids* **35-36**, 543 (1980).

⁹S. A. Solin, N. Wada and J. Wong, in *Amorphous Carbon and Its Structural Relationship to Amorphous Silicon and Germanium*, Vol. 43 of the Institute of Physics Conference Series, edited by B. L. H. Wilson (IOP, London, 1979), p. 721.

¹⁰B. S. Elman, M. S. Dresselhaus, H. Mazurek and M. Shaygan, *Phys. Rev. B* **25**, 4142 (1982).

¹¹Workshop on Diamondlike Carbon Films: April 19 and 20, 1982, EDM Corporation, Albuquerque, New Mexico (unpublished).

¹²M. DiDomenico, Jr., S. H. Wemple, S. P. S. Porto, and R. P. Bauman, *Phys. Rev.* 174, 522 (1968).

¹³R. P. Vidano and D. B. Fishbach, in *Extended Abstracts of the 15th Biennial Conference on Carbon, 1981*, edited by F. L. Vogel and W. C. Foresman (American Carbon Society, University Park, Penn., 1981), p. 468; R. P. Vidano, Ph.D. thesis, University of Washington, 1980.